

**Accelerated evolution of an *Lhx2* enhancer shapes
mammalian social hierarchies**

Yuting Wang, Guangyi Dai, Zhili Gu, Guopeng Liu, Ke Tang, Yi-Hsuan Pan, Yujie Chen, Xin Lin, Nan Wu, Haoshan Chen, Su Feng, Shou Qiu, Hongduo Sun, Qian Li, Chuan Xu, Yanan Mao, Yong Edward Zhang, Philipp Khaitovich, Yan-Ling Wang, Qunxiu Liu, Jing-Dong Jackie Han, Zhen Shao, Gang Wei, Chun Xu, Naihe Jing, Haipeng Li

Supplementary text

Figures S1 to S15

Tables S1 to S10

SI References

Supplementary Information Text

Motor Coordination, Balance

Results of the rota-rod test¹ revealed that no significant difference in motor coordination and balance between PAS1^{c/c} and PAS1^{c/m}, and between PAS1^{/m} and PAS1^{-/-} male mice (Two-tailed permutation test, $P = 0.914$, and 0.394 , respectively) (Supplementary information, Fig. S13). However, a significant difference in motor coordination and balance was observed between PAS1^{w/m} and PAS1^{w/w} male mice (Two-tailed permutation test, $P = 0.030$). Results of the pole test² showed that all 3 pairs of male mice had no significant difference in motor coordination and balance (Supplementary information, Fig. S13) (Two-tailed permutation test, $P = 0.972$, 0.076 , and 0.996 , respectively).

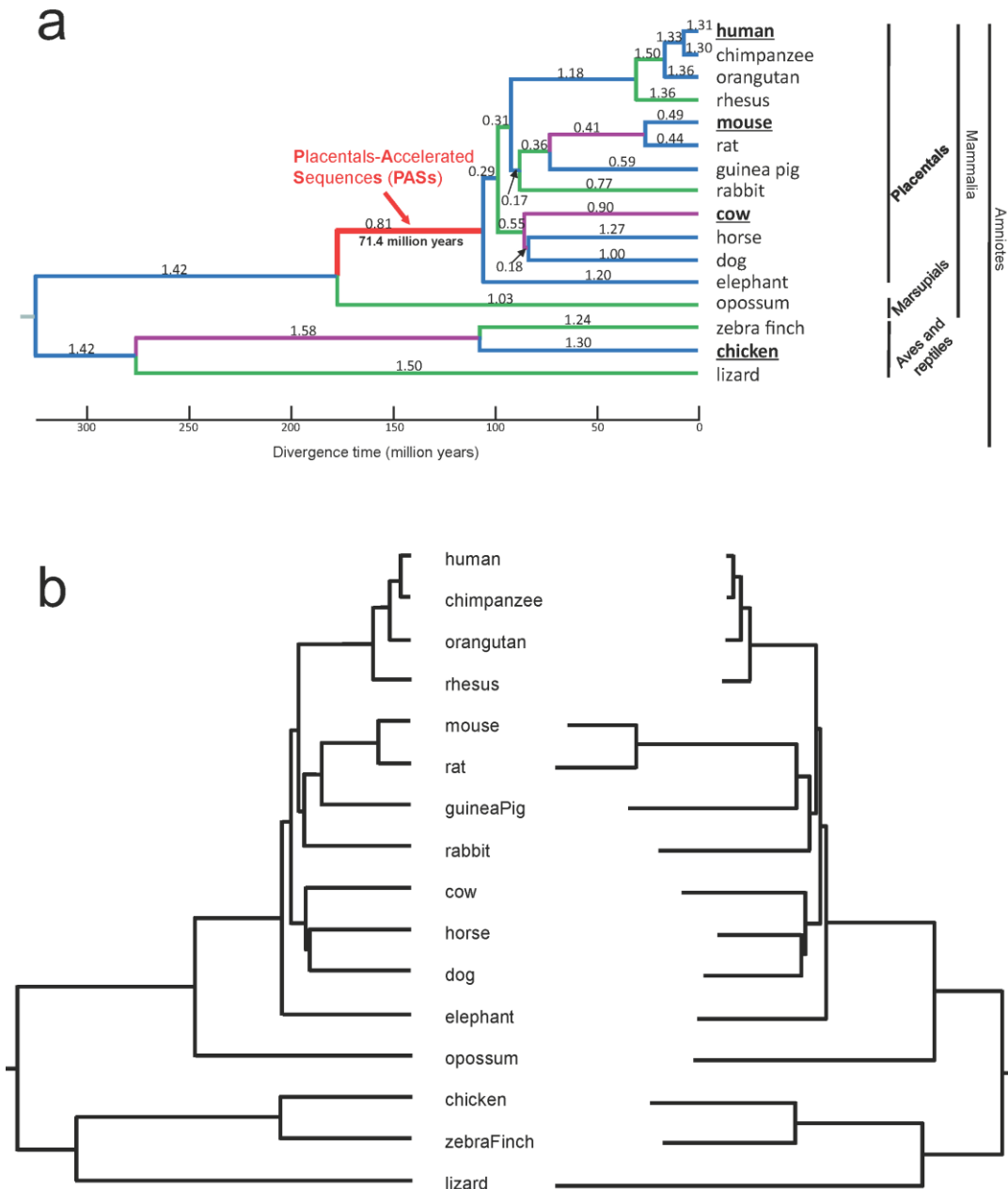


Fig. S1. Phylogenetic tree of 16 amniotes for studying placental-accelerated sequences (PASs).

(a) The branch sets of tree and the branch-specific normalization factors. Connected branches with the same color (excluding the red branch) were considered as a branch set. There were 17 branch sets. The average evolutionary rate of each window in each branch set was calculated. The local evolutionary rate of the i -th branch was normalized by the branch-specific normalization factor α_i . α_i was shown above the branch. The normalization factors are larger than 1.0 for primates and smaller than 1.0 for rodents, consistent with the previous conclusions of slow-evolving primates and fast-evolving rodents.³

(b) Comparison between the original phylogenetic tree (left) and the reconstructed neighbor-joining tree⁴ based on the genome-wide alignments using the eGPS software (right).⁵

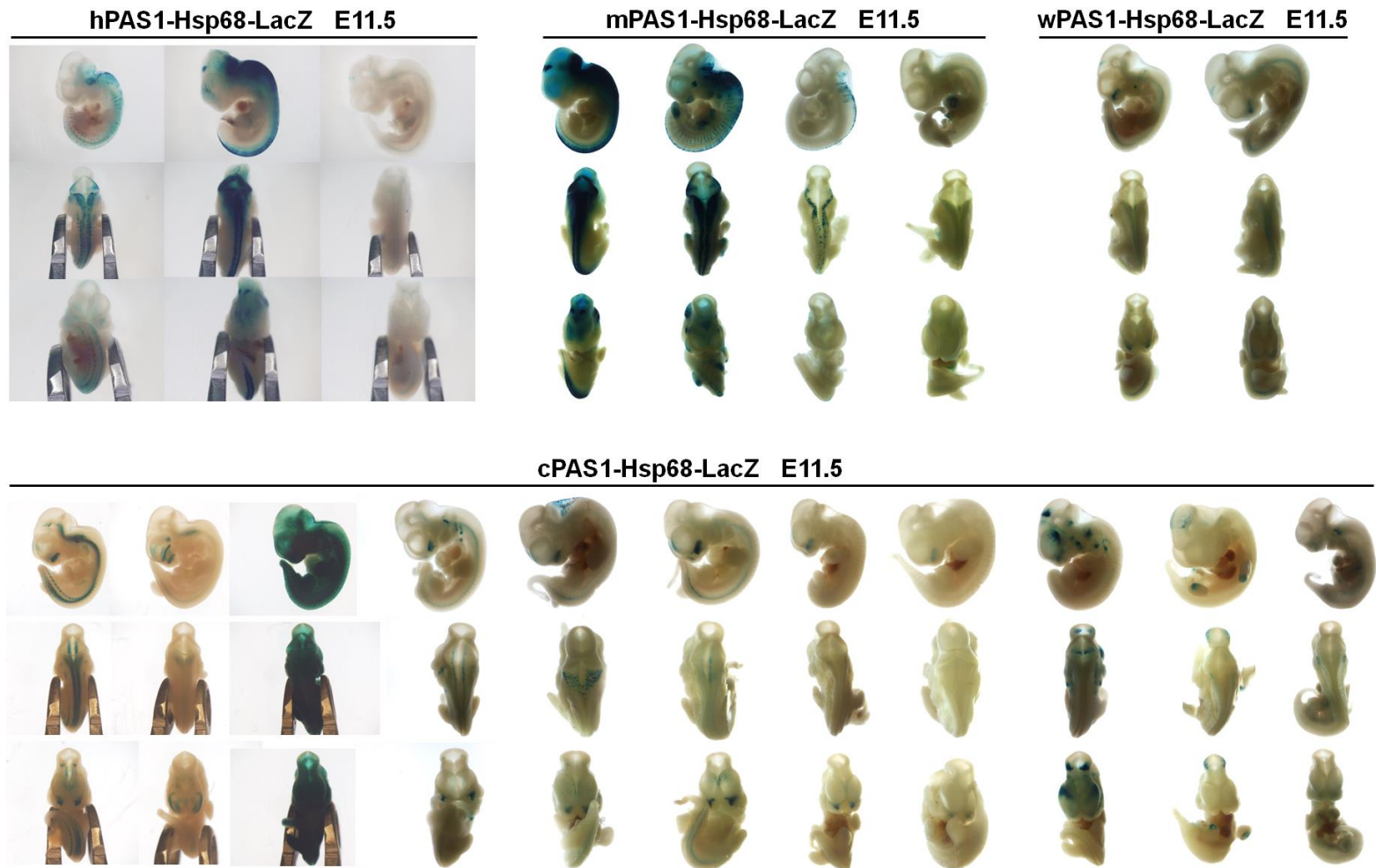


Fig. S2. LacZ-positive E11.5 embryos from hPAS1, mPAS1, wPAS1, and cPAS1 transgenic mouse enhancer assays. Lateral (upper), dorsal (middle), and ventral (bottom) views of all embryos are shown. The second mPAS1-Hsp68-LacZ embryo, the first wPAS1-Hsp68-LacZ embryo, and the sixth cPAS1-Hsp68-LacZ embryo were presented in Figure 2c.

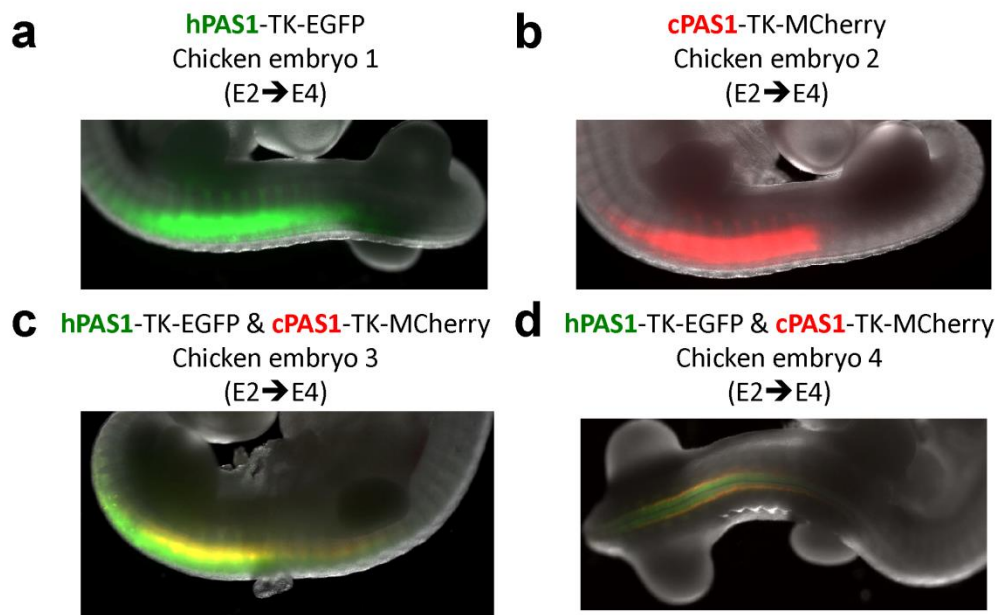


Fig. S3. Effect of hPAS1 and cPAS1 on the expression of the fluorescent protein gene in the spinal cord of chicken embryo.

(a) and (b): E4 chicken embryos after electroporation of hPAS1-TK-EGFP (green) or cPAS1-TK-mCherry (red) plasmid into the neural tube of E2 chicken embryos. Both EGFP and mCherry fluorescence signals were detected in the spinal cord of chicken embryos.

(c) and (d): Co-expression of EGFP (green) and mCherry (red) in the neural tube of chicken embryos after electroporation of hPAS1-TK-EGFP and cPAS1-TK-mCherry plasmids at 1:1 ratio.

(a, b, c) lateral view (d) dorsal view. The TK promoter is a minimal promoter and does not drive the expression of the reporter genes without an enhancer.

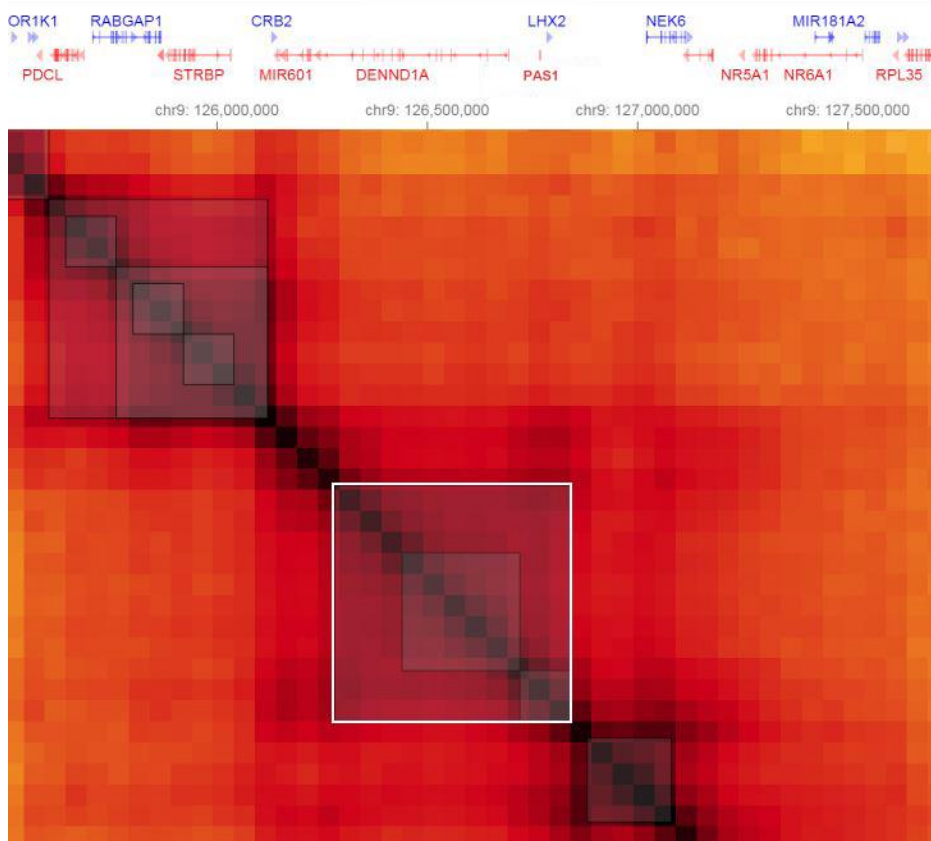


Fig. S4. Identification of topologically associating domain (TAD) around PAS1. The TAD was determined by TADTree,⁶ and indicated with an empty square. The TAD was taken as the boundary of the region to which PAS1 may act. Data were obtained from.⁷

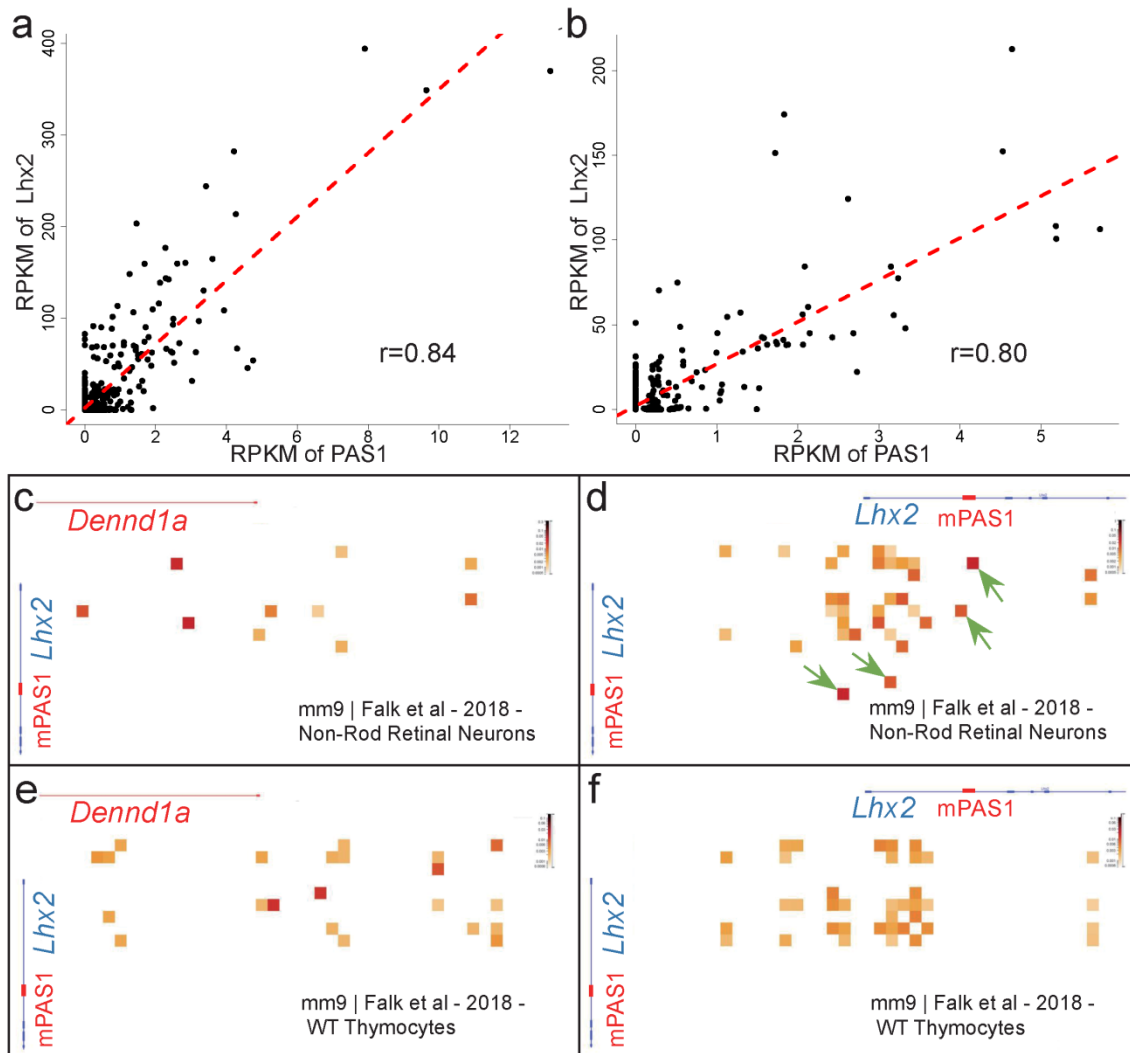


Fig. S5. Evidences for PAS1 regulating the expression of the *Lhx2* gene.

(a) Positive correlation between the CAGE signals of PAS1 and *Lhx2* expression in mouse samples. $P < 2.2 \times 10^{-16}$. The publicly available data were obtained from FANTOM. RPKM: Reads per kilobase per million mapped reads.

(b) Positive correlation between the CAGE signals of PAS1 and *Lhx2* expression in human samples. $P < 2.2 \times 10^{-16}$. The publicly available data were obtained from FANTOM. RPKM: Reads per kilobase per million mapped reads.

(c) – (f) Hi-C signals of PAS1 and *Lhx2* TSS in different mouse cell lines.⁸ Hi-C signals (green arrow heads) were observed on PAS1 and *Lhx2*, but not on PAS1 and *Dennd1a* (C, and D); No Hi-C signal was detected in non-neural cells (E, and F)

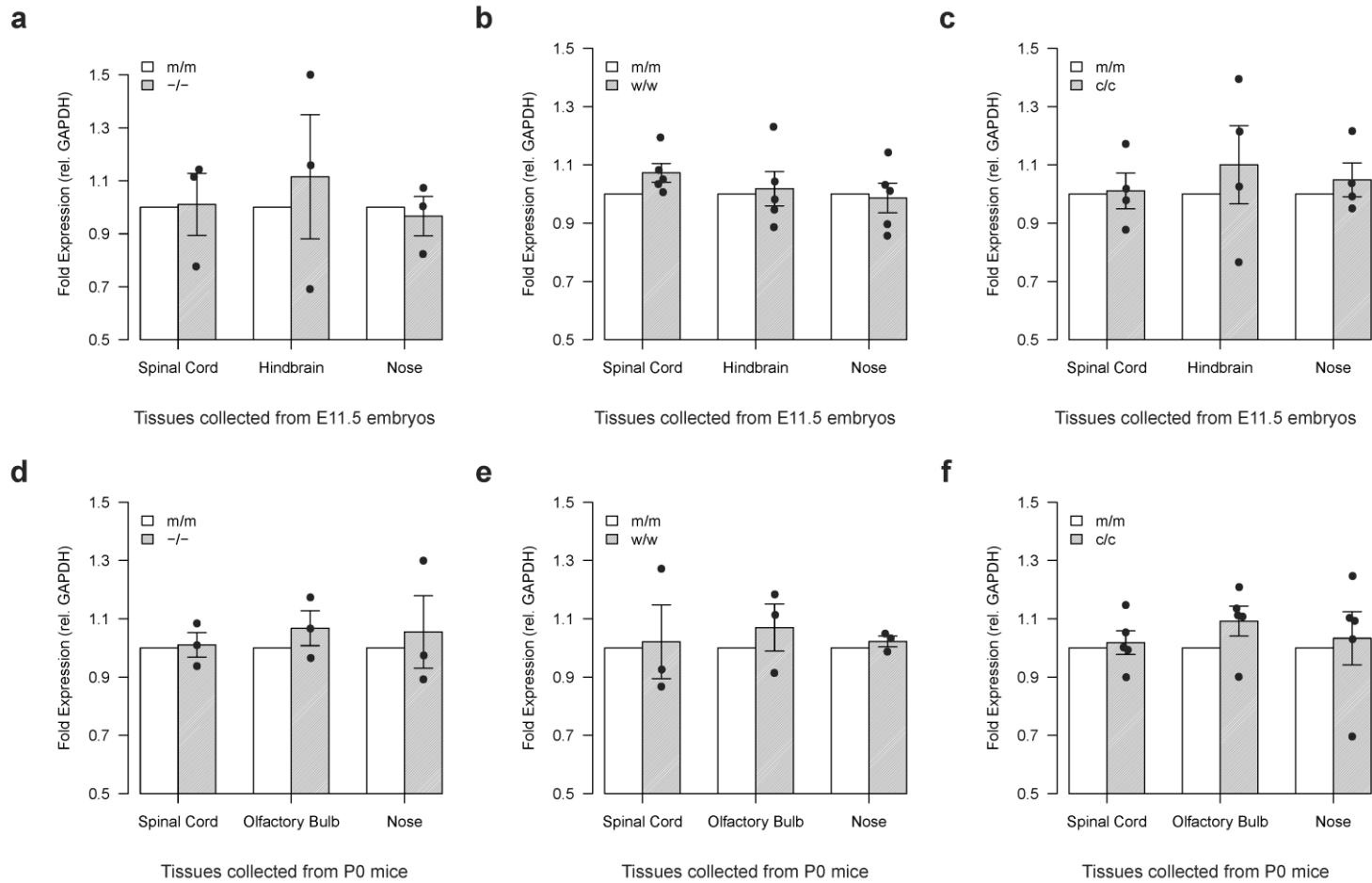


Fig. S6. mRNA levels of *Dennd1a* in E11.5 embryos (a–c) and P0 (d–f) of *PAS1*^{-/-}, *PAS1*^{w/w} and *PAS1*^{c/c} mice compared with those of wide-type littermates. mRNA levels of *Dennd1a* determined by RT-qPCR were normalized to those of *Gapdh*. Error bars represent the s.e.m of at least three biological replicates and three technical replicates for each experiment.

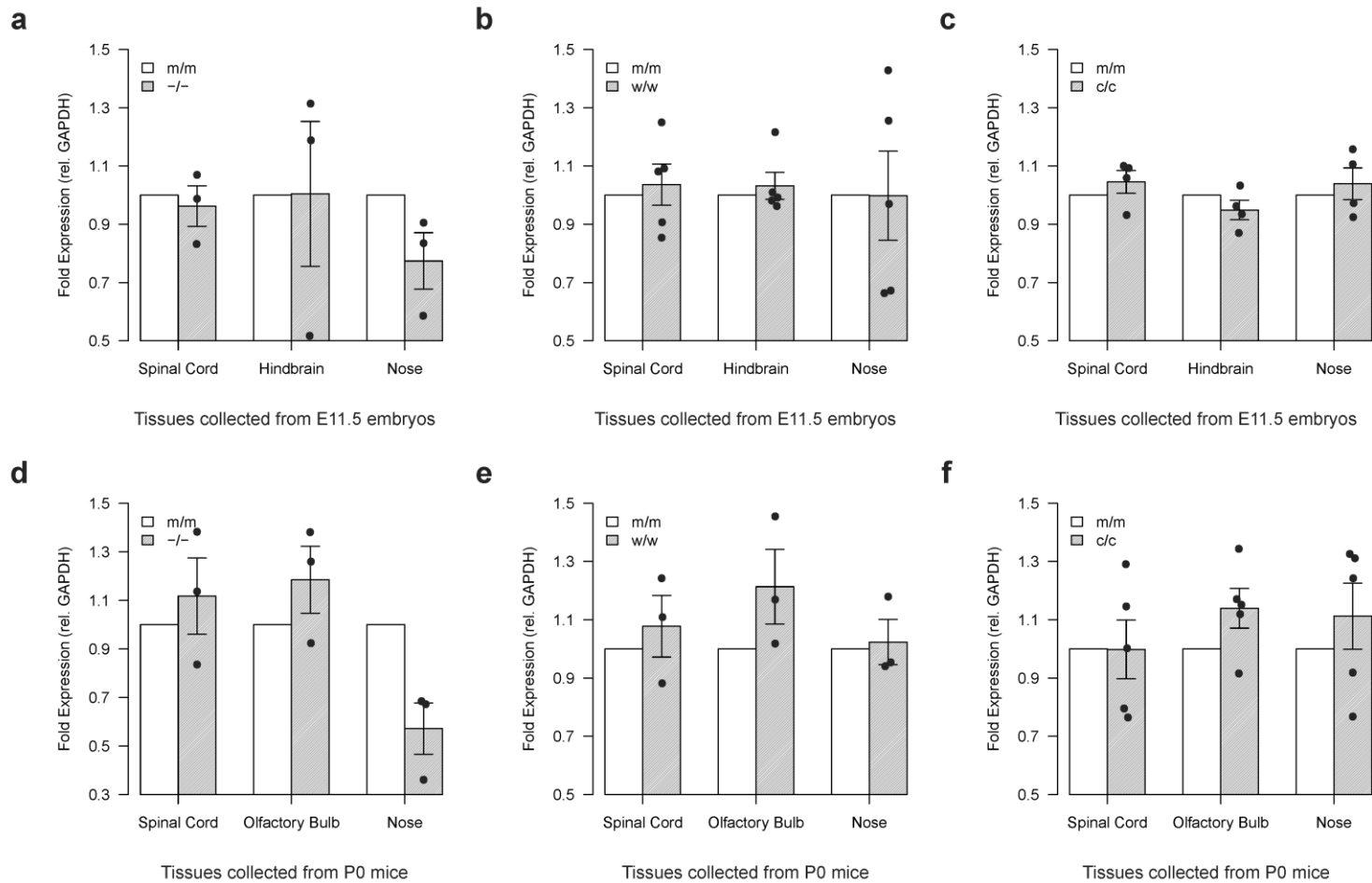


Fig. S7. mRNA levels of *Gm27197* in E11.5 embryos(a-c) and P0(d-f) of *PAS1*^{-/-}, *PAS1*^{w/w}, *PAS1*^{c/c} mice compared with those of wide-type littermates. mRNA levels of *Gm27197* determined by RT-qPCR were normalized to those of *Gapdh* gene. Error bars represent the s.e.m from at least three biological replicates with three technical replicates for each experiment.

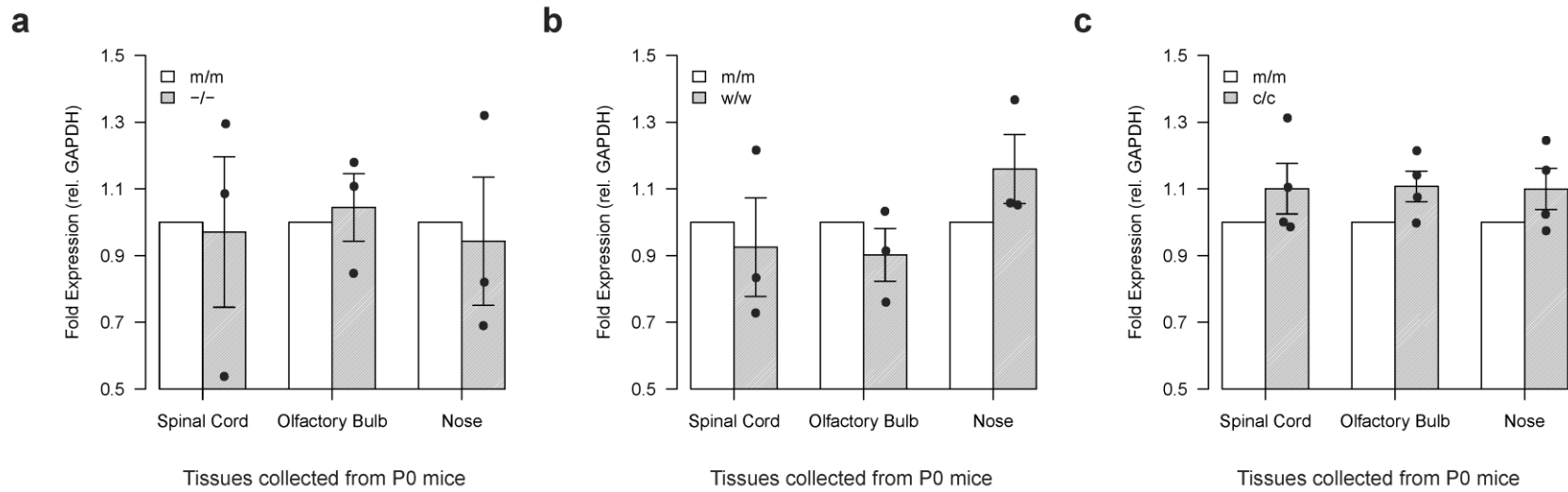


Fig. S8. *Lhx2* mRNA levels determined by RT-qPCR in P0 of $PAS1^{-/-}$, $PAS1^{w/w}$ and $PAS1^{c/c}$ mice compared with those of wide-type littermates. *Lhx2* mRNA levels were normalized to those of *Gapdh*. Error bars represent the s.e.m of at least three biological replicates (three for $PAS1^{-/-}$, three for $PAS1^{w/w}$, four for $PAS1^{c/c}$) and three technical replicates for each experiment.

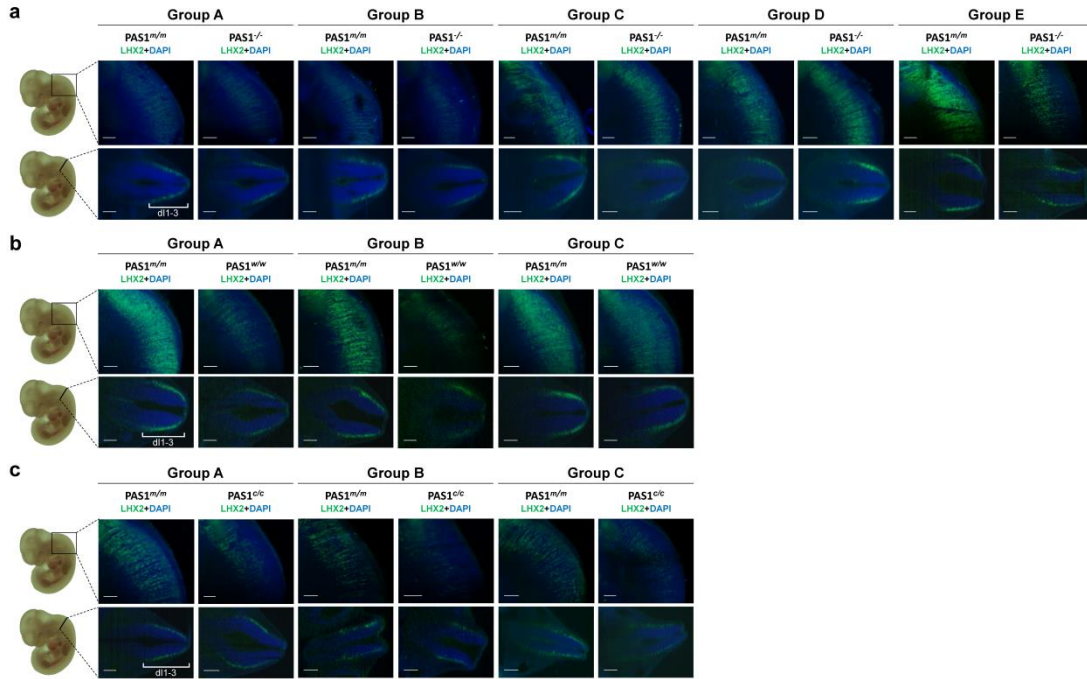


Fig. S9. Effect of PAS1s on the expression of *Lhx2* in the primitive spinal cord. E11.5 $PAS1^{-/-}$, $PAS1^{w/w}$, $PAS1^{c/c}$ and wild-type mouse embryos were immuno-stained for LHX2 (green) after CUBIC clearing. The region in which *Lhx2* was expressed in the wild-type ($PAS1^{m/m}$) embryo is marked (dII-3, three neuronal cell types).⁹ For each mouse strain, at least three groups of embryos were examined. Each group of embryos had two age-matched littermates of specific PAS1 genotypes. Scale bar, 200 μm .

(a) Five groups of $PAS1^{m/m}$ and $PAS1^{-/-}$ pair.

(b) Three groups of $PAS1^{m/m}$ and $PAS1^{w/w}$ pair. The $PAS1^{m/m}$ embryo in Group A was used in Figure 3H as the wild-type control.

(c) Three groups of $PAS1^{m/m}$ and $PAS1^{c/c}$ pair.

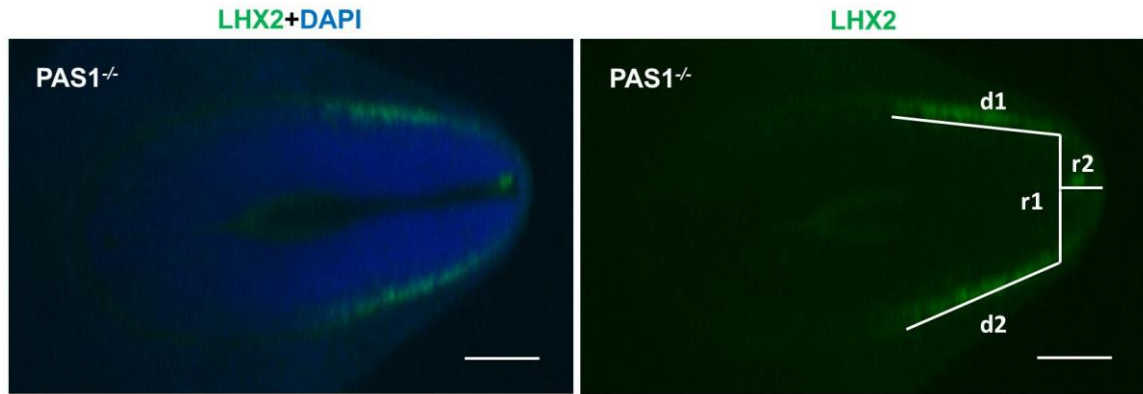


Fig. S10. Schematic of four summary statistics used for examination of LHX2 expression in spinal cord sections. d1 and d2 define the width of the areas in which the LHX2 protein was expressed, r1 and r2 denote the distances of the areas with LHX2 protein expression away from the dorsal vertex of the spinal cord. Scale bar, 200 μ m.

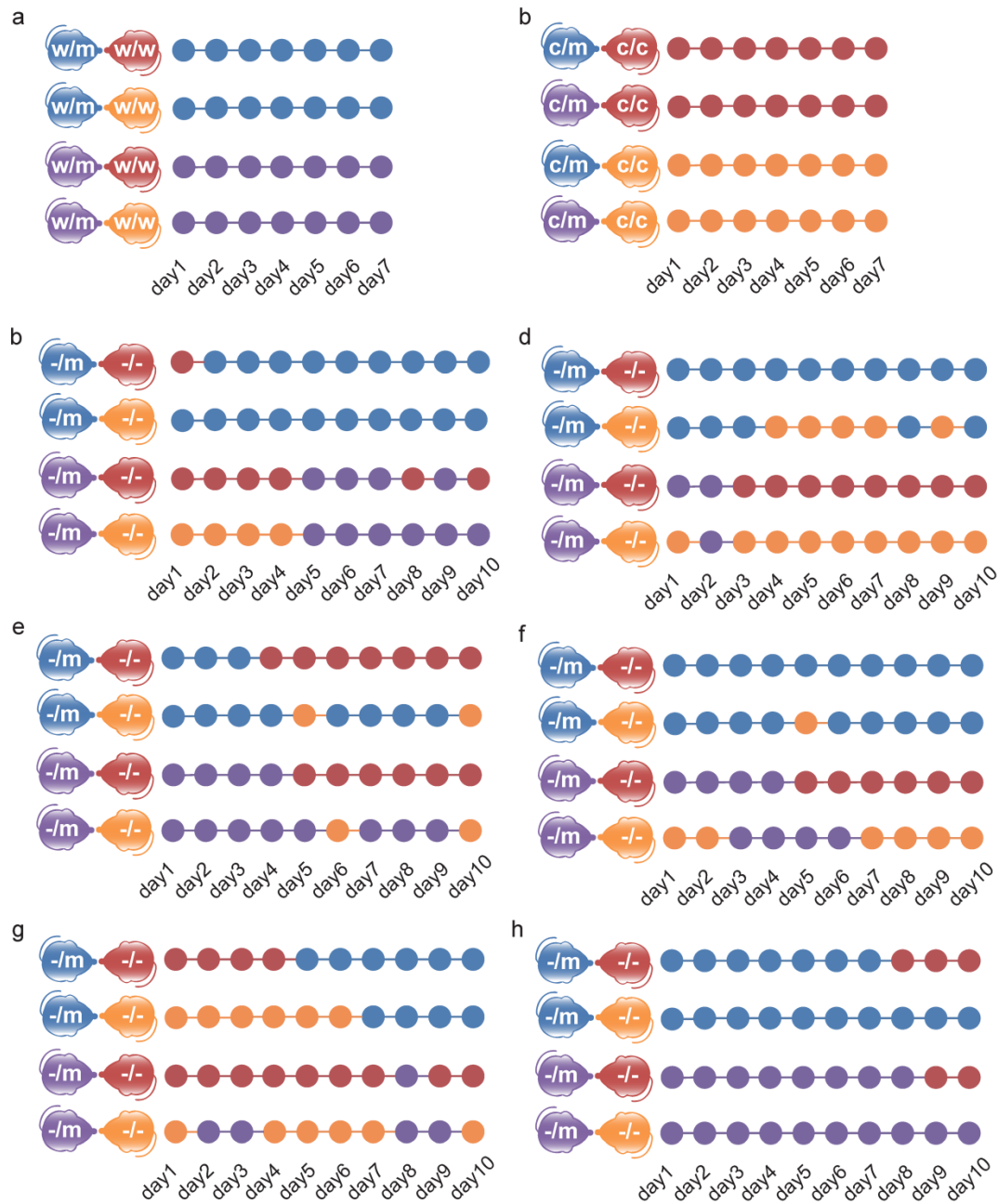


Fig. S11. Stability of tube test ranks.

The social dominance tube test was performed daily for 7 to 10 consecutive days. The winner of each test is indicated with a colored dot, which represents a specific *PAS1* genotype of the mice tested. Day1 indicates the first tube test trial after the three-day training. Please note that we applied the tube test only to cage mice living together for at least 2 weeks (Table S5-7).

(a) Tests of *PAS1*^{w/m} vs. *PAS1*^{w/w} male mice. All winners were of the *PAS1*^{w/m} genotype.

(b) Tests of *PAS1*^{c/m} vs. *PAS1*^{c/c} male mice. All winners were of the *PAS1*^{c/c} genotype.

(c, d, e, f, g, h) Tests of *PAS1*^{-/m} vs. *PAS1*^{-/-} male mice. The genotype of the winner varied.

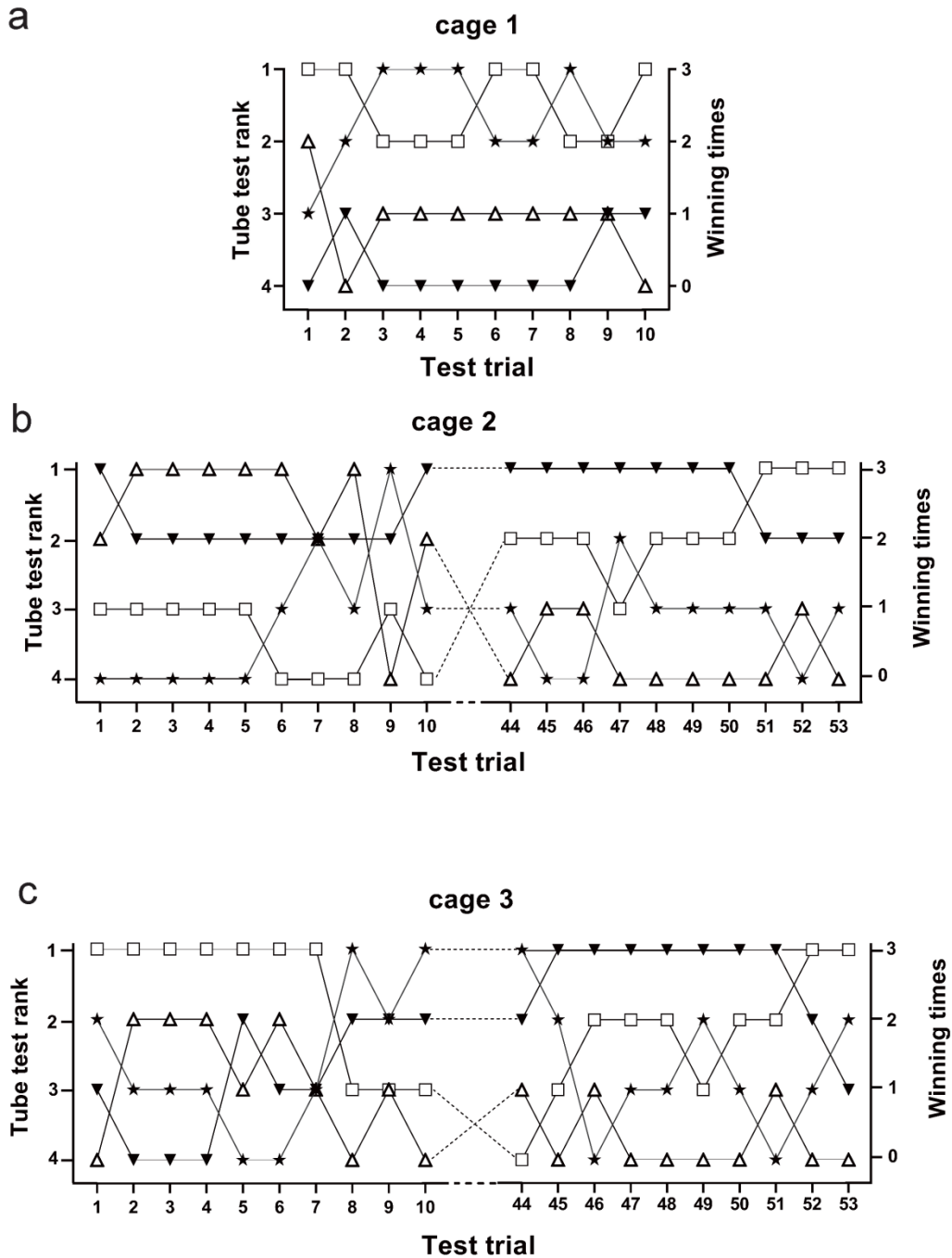


Fig. S12. $PAS1^{-/-}$ male mice lack social stratification.

The detailed information of $PAS1^{-/-}$ mice caged together was provided in Table S8.

(a) The social dominance tube test was performed daily for 10 consecutive days.

(b, c) The social dominance tube test was performed 20 times (once per day) within 53 consecutive days.

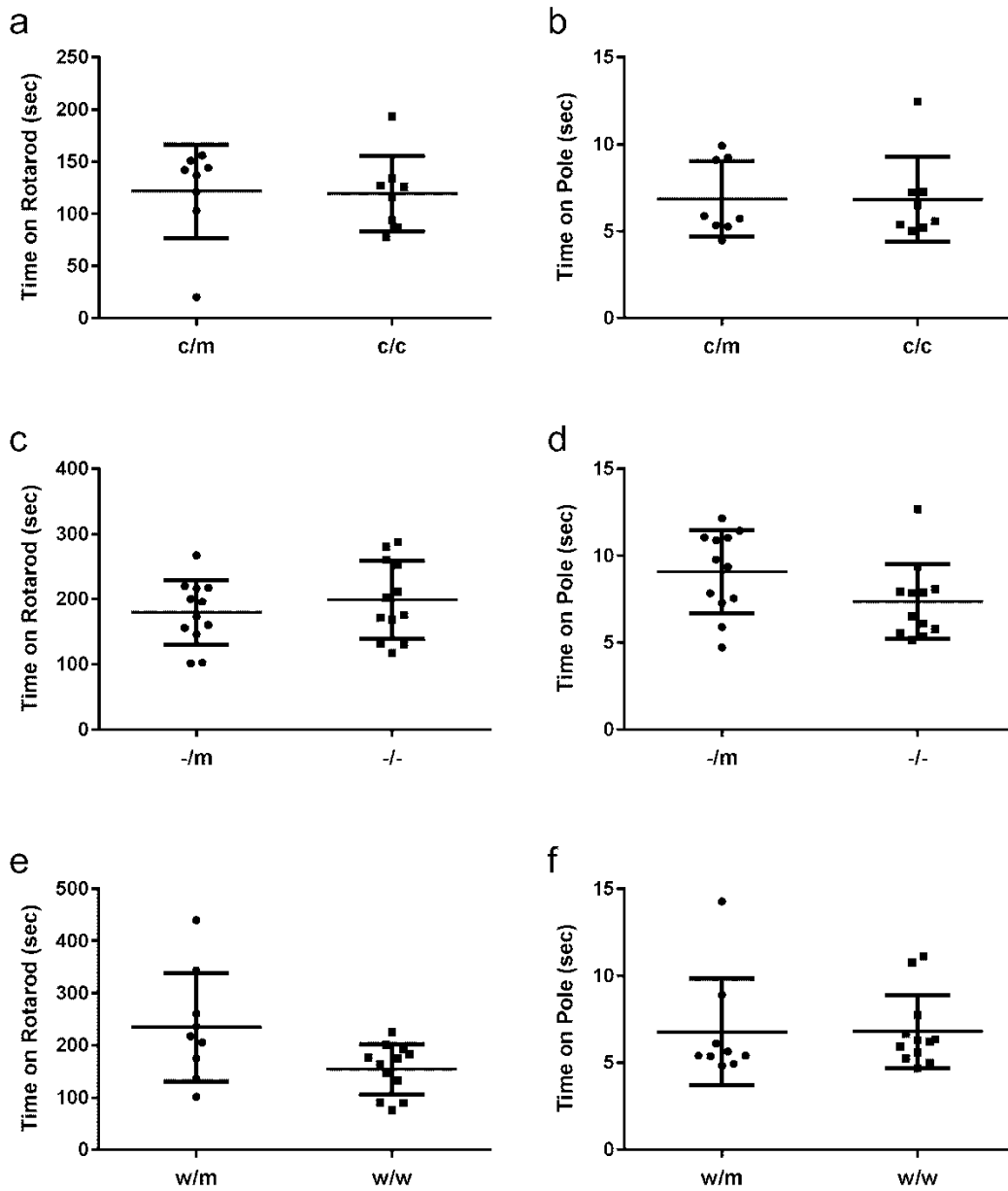


Fig. S13. Motor and activity tests. Data are presented as mean \pm SD.

- (a) Rota-rod tests of $PAS1^{c/m}$ ($n=8$) and $PAS1^{c/c}$ ($n=8$) mice.
- (b) Pole tests of $PAS1^{c/m}$ ($n=8$) and $PAS1^{c/c}$ ($n=8$) mice
- (c) Rota-rod tests of $PAS1^{-/m}$ ($n=12$) and $PAS1^{-/-}$ ($n=12$) mice.
- (d) Pole tests of $PAS1^{-/m}$ ($n=12$) and $PAS1^{-/-}$ ($n=12$) mice.
- (e) Rota-rod tests of $PAS1^{w/m}$ ($n=9$) and $PAS1^{w/w}$ ($n=12$) mice.
- (f) Pole tests of $PAS1^{w/m}$ ($n=9$) and $PAS1^{w/w}$ ($n=12$) mice.

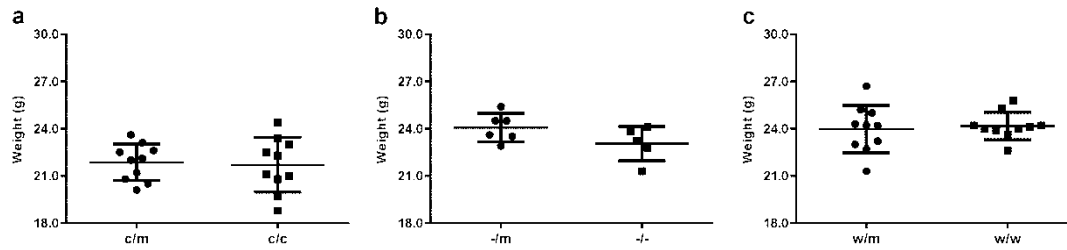
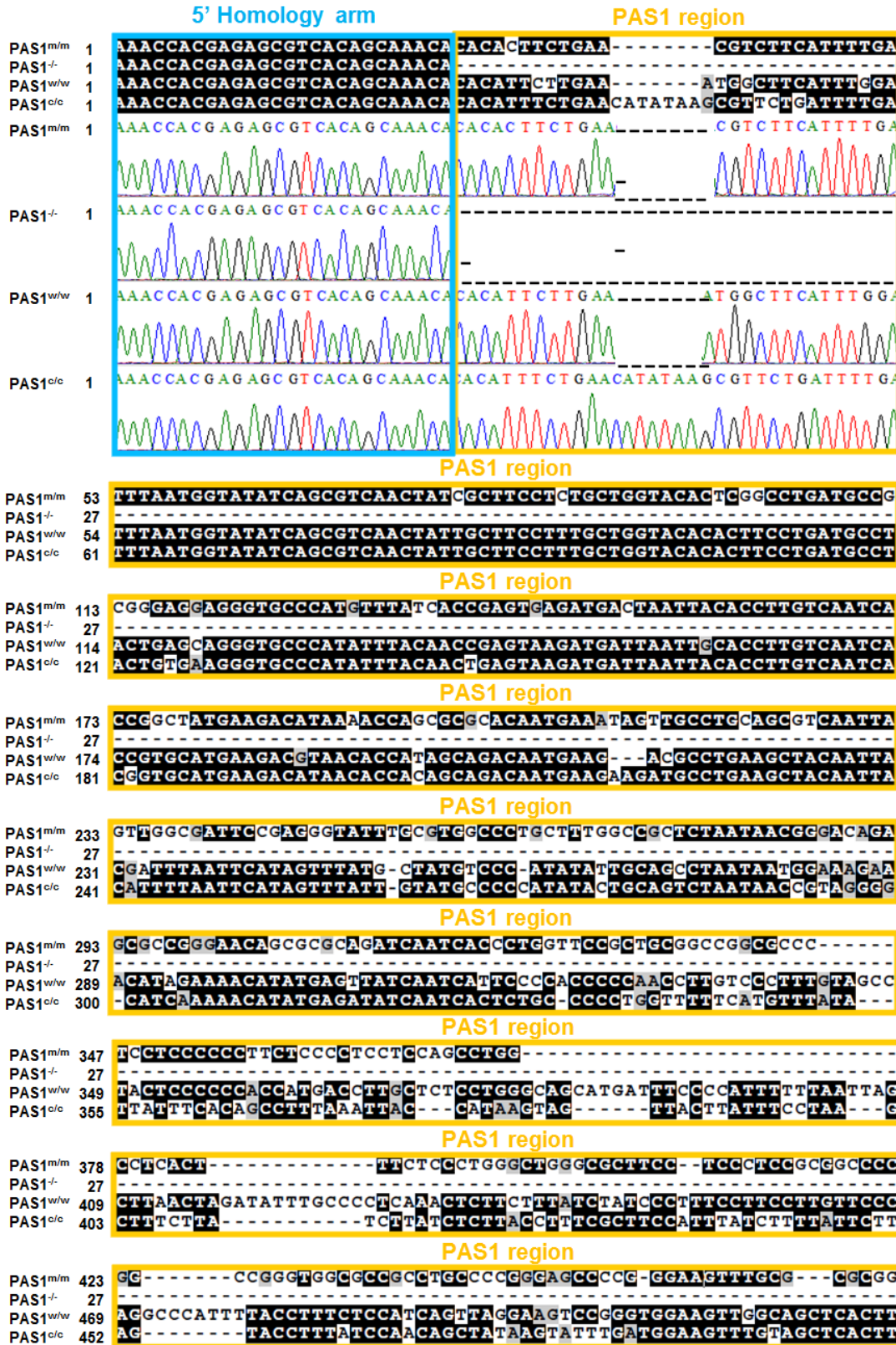


Fig. S14. Body weight of mice at two months (before group-housing). Data are presented as mean \pm SD.

(a) Body weight of PAS1^{c/m} ($n=10$) and PAS1^{c/c} mice ($n=10$) at 9.0-10.0 weeks of age. One-way analysis of variance $P = 0.822$.

(b) Body weight of PAS1^{-/m} ($n=6$) and PAS1^{-/-} mice ($n=5$) at 9.4-10.4 weeks of age. One-way analysis of variance $P = 0.122$.

(c) Body weight of PAS1^{w/m} ($n=10$) and PAS1^{w/w} mice ($n=10$) at 9.5-10.5 weeks of age. One-way analysis of variance $P = 0.734$.



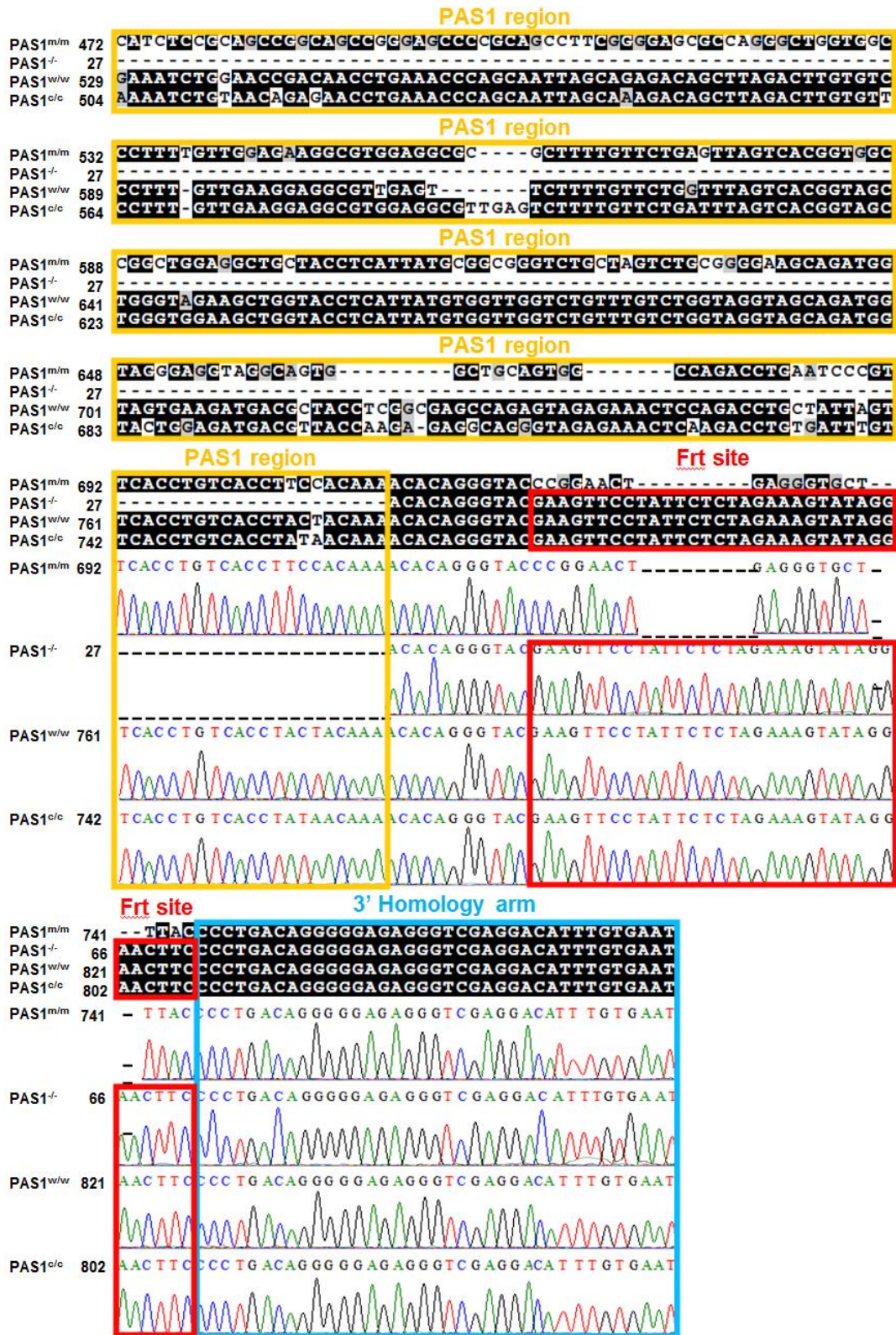


Fig. S15. Alignments of nucleotide sequences of *PAS1^{m/m}* (wild-type), *PAS1^{-/-}*, *PAS1^{w/w}* and *PAS1^{c/c}* mice.

Table S1. List of the accelerated regions in the ancestral lineage of placental mammals. Genomic locations of accelerated regions and the most adjacent protein coding genes were determined by searching the Ensembl/Havana database (GRCh37). The threshold of P -values was 3.06×10^{-9} after Bonferroni correction. H3K27ac signals¹⁰ within 30-kb regions were obtained from ENCODE/LICR on the UCSC genome browser with a vertical viewing range of [0.2, 10]. The accelerated regions are marked with inverted triangle, located in the middle of the 30-kb regions. Median gene expression levels in 51 tissues and 2 cell lines, based on RNA-seq data of 8,555 tissue samples from 570 adult post-mortem individuals from the NIH Genotype-Tissue Expression (GTEx) project (V6, October 2015),¹¹ were visualized with UCSC genome browser. GTEx gene expression levels were log-transformed. Green circle – Passed related filters; Black circle – Failed to pass related filters.

Rank	Coordinates	Genomic Location	Closest Coding Genes	P -value	Active enhancer signal (H3K27ac) in whole mouse brain E14.5	GTEx Gene Expression in 53 adult human tissues (Brain in yellow)
1	hg19 chr9:126770941-126771040 mm9 chr2:38203835-38203933	Non-coding	<i>Lhx2</i>	3.15×10^{-18}		
2	hg19 chr9:126770921-126771020 mm9 chr2:38203815-38203913	Non-coding	<i>Lhx2</i>	5.94×10^{-18}		
3	hg19 chr9:126770901-126771000 mm9 chr2:38203795-38203894	Non-coding	<i>Lhx2</i>	7.14×10^{-18}		
4	hg19 chr9:126770961-126771060 mm9 chr2:38203855-38203953	Non-coding	<i>Lhx2</i>	2.77×10^{-18}		
5	hg19 chr11:8310741-8310840 mm9 chr2:160352318-160352420	intergenic	<i>Lmo1</i>	9.63×10^{-13}		
6	hg19 chr9:126771021-126771120 mm9 chr2:38203914-38204013	Non-coding	<i>Lhx2</i>	1.92×10^{-12}		
7	hg19 chr20:39498201-39498300 mm9 chr2:160352318-160352420	intergenic	<i>Top1</i>	2.78×10^{-11}		
8	hg19 chr9:126770601-126770700 mm9 chr2:38203489-38203588	Non-coding	<i>Lhx2</i>	8.28×10^{-11}		
9	hg19 chr20:57485821-57485920 mm9 chr2:174171826-174171924	coding	<i>Gnas</i>	1.26×10^{-10}		
10	hg19 chr9:126770541-126770640 mm9 chr2:38203429-38203528	Non-coding	<i>Lhx2</i>	3.15×10^{-10}		
11	hg19 chr9:126770641-126770740 mm9 chr2:38203529-38203629	Non-coding	<i>Lhx2</i>	3.84×10^{-10}		
12	hg19 chr3:71113981-71114080 mm9 chr6:98978164-98978259	intronic	<i>Foxp1</i>	5.27×10^{-10}		
13	hg19 chr3:71114041-71114140 mm9 chr6:98978223-98978313	intronic	<i>Foxp1</i>	5.48×10^{-10}		
14	hg19 chr4:1804621-1804720	coding	<i>Fgfr3</i>	5.95×10^{-10}		

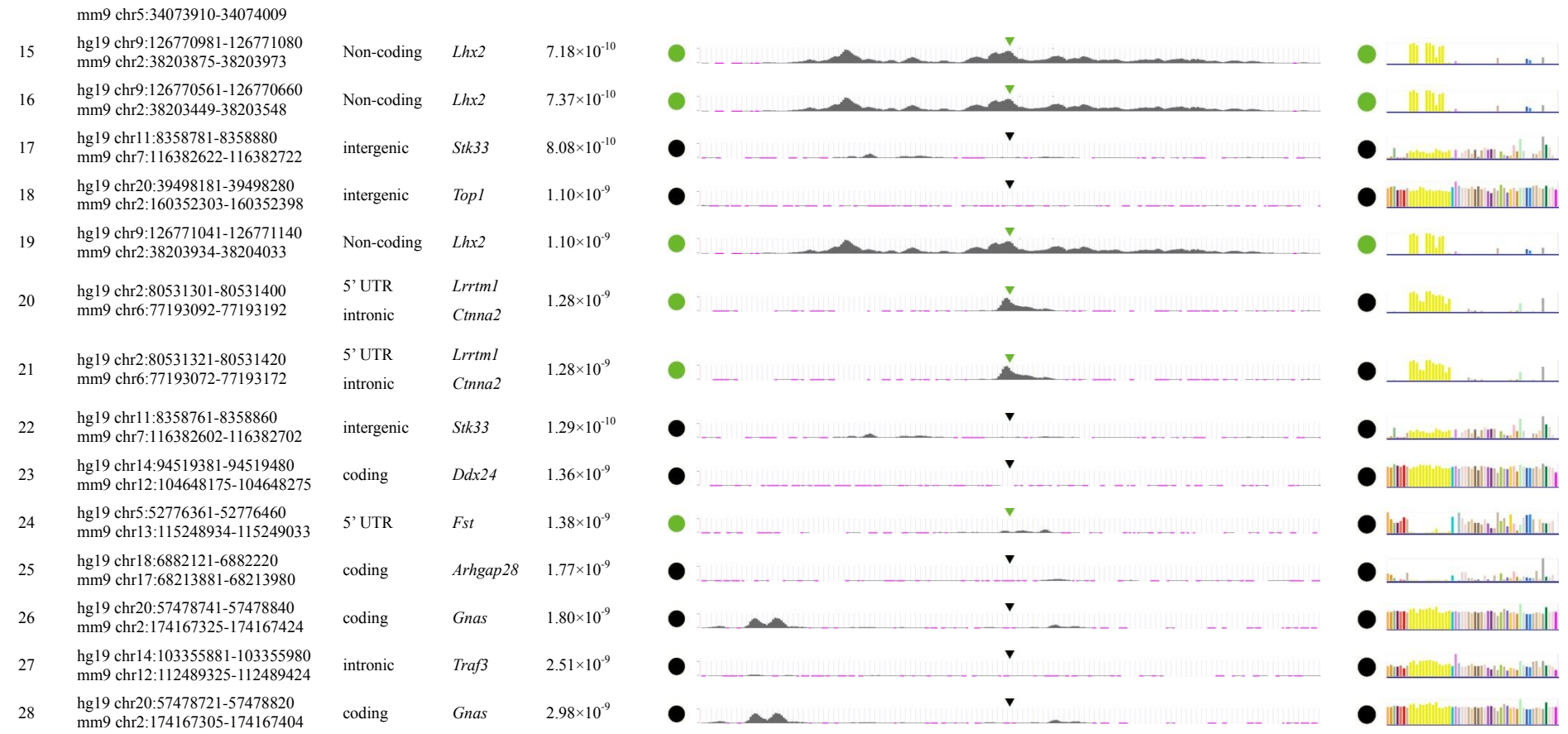


Table S2. Summary statistics of *Lhx2* gene expression levels in spinal cord sections of PAS1^{-/-} E11.5 mouse embryos. Images of spinal cord sections of E11.5 PAS1^{m/m} (wild-type) and PAS1^{-/-} embryos immuno-stained for LHX2 after CUBIC clearing were captured and analyzed with the Vision4D software (version 2.12.3, Arivis). Five groups of embryos were examined, and each group of embryos was from age-matched littermates. Three consecutive sections of each embryo were examined. d1 and d2 define the width of the areas with LHX2 protein expression. r1 and r2 denote the distances of the areas with LHX2 protein expression away from the dorsal vertex of the spinal cord. Measurements were conducted by two experts independently, and results are presented in the following two sub-tables. Two-tailed permutation test was used, **P* < 0.05, ***P* < 0.01.

		Group A		Group B		Group C		Group D		Group E		P-value
		PAS1 ^{m/m}	PAS1 ^{-/-}	PAS1 ^{m/m}	PAS1 ^{-/-}	PAS1 ^{m/m}	PAS1 ^{-/-}	PAS1 ^{m/m}	PAS1 ^{-/-}	PAS1 ^{m/m}	PAS1 ^{-/-}	
Expert 1												
d1 (μ m)	Section1	539.56	430.83	494.04	439.24	484.56	467.70	460.42	370.85	582.06	482.09	0.00001 **
	Section2	507.35	417.62	477.64	427.49	470.54	462.40	444.07	396.12	537.89	420.00	
	Section3	559.73	410.76	531.60	416.65	481.26	464.10	448.82	270.45	532.01	407.67	
d2 (μ m)	Section1	608.89	496.80	536.04	416.15	506.87	497.80	468.25	383.84	581.28	505.56	0.00004 **
	Section2	567.11	494.62	580.97	463.60	484.77	487.69	461.89	417.95	535.26	509.69	
	Section3	574.08	434.10	564.94	416.18	541.19	434.00	425.55	377.96	510.70	444.90	
r1 (μ m)	Section1	253.62	315.56	253.62	333.43	152.09	285.81	131.75	356.98	489.63	395.94	0.00445 **
	Section2	242.13	352.30	242.13	314.31	166.74	297.59	167.84	318.95	474.67	370.93	
	Section3	260.09	353.08	260.09	351.72	159.37	277.10	126.43	360.40	433.02	377.27	
r2 (μ m)	Section1	61.72	137.31	61.72	142.46	27.94	111.96	35.57	108.26	68.50	163.00	0.00003 **
	Section2	63.81	116.90	63.81	139.78	48.28	107.39	43.19	120.51	66.07	157.50	
	Section3	66.06	116.73	66.06	172.94	53.35	101.81	43.19	118.32	64.65	170.30	
Expert 2												
d1 (μ m)	Section1	529.66	431.91	482.04	430.18	478.68	455.64	472.13	350.64	583.06	470.67	0.00004 **
	Section2	543.56	411.86	539.55	421.66	498.29	382.47	478.54	469.43	627.06	460.97	
	Section3	575.63	372.20	765.87	417.68	493.55	451.34	439.37	300.39	574.94	468.98	
d2 (μ m)	Section1	656.01	442.12	545.45	406.20	552.24	502.86	518.37	459.56	604.80	510.91	0.00001 **
	Section2	578.58	511.04	614.04	520.80	509.50	478.95	425.55	412.17	571.81	526.14	
	Section3	613.61	373.40	604.75	470.22	564.01	424.54	441.14	414.47	475.52	414.73	
r1 (μ m)	Section1	259.98	346.97	199.36	328.92	199.32	279.94	121.89	310.39	532.40	396.75	0.00401 **
	Section2	266.80	314.83	205.22	324.53	172.68	296.50	143.62	282.44	475.38	365.27	
	Section3	235.67	366.30	153.75	269.73	148.15	281.83	113.28	326.01	434.92	373.14	
r2 (μ m)	Section1	63.51	140.30	67.27	158.72	47.56	106.71	43.19	135.19	90.75	183.27	0.00003 **
	Section2	66.34	108.27	73.68	151.16	56.86	101.81	63.79	115.79	97.32	168.74	
	Section3	55.89	146.72	58.45	106.74	50.01	94.20	45.73	139.38	89.12	186.26	

Table S3. Summary statistics of *Lhx2* gene expression levels in spinal cord sections of PAS1^{w/w} E11.5 mouse embryos. Images of spinal cord sections of E11.5 PAS1^{m/m} (wild-type) and PAS1^{w/w} embryos immuno-stained for LHX2 after CUBIC clearing were captured and analyzed with the Vision4D software (version 2.12.3, Arivis). Three groups of embryos were examined, and each group of embryos was from age-matched littermates. Three consecutive sections of each embryo were examined. d1 and d2 define the width of the areas with LHX2 protein expression. r1 and r2 denote the distances of the areas with LHX2 protein expression away from the dorsal vertex of the spinal cord. Measurements were conducted by two experts independently, and results are presented in the following two sub-tables. Two-tailed permutation test was used, **P* < 0.05, ***P* < 0.01.

		Group A		Group B		Group C		P-value
		PAS1 ^{m/m}	PAS1 ^{w/w}	PAS1 ^{m/m}	PAS1 ^{w/w}	PAS1 ^{m/m}	PAS1 ^{w/w}	
Expert 1								
d1 (μm)	Section1	512.05	446.78	645.23	403.00	532.79	548.83	0.08092
	Section2	558.82	417.99	647.42	397.57	600.04	638.70	
	Section3	556.00	391.57	602.79	380.79	579.55	561.50	
d2 (μm)	Section1	617.43	380.64	648.93	459.64	542.19	626.77	0.08068
	Section2	531.43	462.33	680.30	416.86	575.26	575.73	
	Section3	586.85	444.22	642.15	435.91	544.53	595.07	
r1 (μm)	Section1	539.57	630.17	322.17	342.87	292.01	384.59	0.00465 **
	Section2	487.55	612.02	290.03	305.63	264.44	385.46	
	Section3	447.78	534.52	291.35	359.43	253.72	367.33	
r2 (μm)	Section1	54.82	193.13	45.98	150.92	53.35	119.65	0.00543 **
	Section2	43.66	175.52	53.57	160.98	76.23	122.42	
	Section3	40.28	154.95	53.67	166.35	66.05	96.65	
Expert 2								
d1 (μm)	Section1	629.95	368.60	708.30	446.72	521.27	508.43	0.00513 **
	Section2	554.77	324.79	667.57	431.84	609.81	515.76	
	Section3	630.44	401.84	605.03	353.81	576.36	555.17	
d2 (μm)	Section1	743.56	520.68	680.43	474.58	454.84	652.03	0.00469 **
	Section2	532.03	507.15	664.14	427.24	521.73	512.31	
	Section3	649.75	431.86	669.80	417.93	496.01	611.85	
r1 (μm)	Section1	521.03	630.17	291.93	309.32	297.49	337.34	0.00401 **
	Section2	483.39	621.99	262.32	305.57	242.40	350.87	
	Section3	445.59	528.85	236.00	335.22	231.50	333.03	
r2 (μm)	Section1	76.11	155.01	73.56	180.61	92.12	121.37	0.00551 **
	Section2	70.72	167.68	73.12	168.56	78.97	129.87	
	Section3	68.70	150.88	66.70	182.32	84.23	114.84	

Table S4. Summary statistics of *Lhx2* gene expression levels in spinal cord sections of PAS1^{c/c} E11.5 mice embryos. Images of spinal cord sections of E11.5 PAS1^{m/m} (wild-type) and PAS1^{c/c} embryos immuno-stained for LHX2 after CUBIC clearing were captured and analyzed with the Vision4D software (version 2.12.3, Arivis). Three groups of embryos were collected, and each group of embryos was from age-matched littermates. Three consecutive sections of each embryo were examined. d1 and d2 define the width of the areas with LHX2 protein expression. r1 and r2 denote the distances of the areas with LHX2 protein expression away from the dorsal vertex of the spinal cord. Measurements were conducted by two experts independently, and results are presented in the following two sub-tables. Two-tailed permutation test was used, **P* < 0.05, ***P* < 0.01.

		Group A		Group B		Group C		P-value
		PAS1 ^{m/m}	PAS1 ^{c/c}	PAS1 ^{m/m}	PAS1 ^{c/c}	PAS1 ^{m/m}	PAS1 ^{c/c}	
Expert 1								
d1 (μ m)	Section1	447.39	329.85	613.81	340.18	548.26	454.95	0.00561 **
	Section2	360.18	300.99	552.89	425.39	578.09	402.69	
	Section3	395.50	279.46	570.85	382.50	554.51	434.37	
d2 (μ m)	Section1	479.68	402.71	630.48	321.16	603.36	463.33	0.00527 **
	Section2	420.08	380.98	547.54	414.26	585.54	481.43	
	Section3	368.65	300.09	577.24	445.73	528.37	482.88	
r1 (μ m)	Section1	97.26	258.24	336.25	458.48	156.00	320.50	0.00492 **
	Section2	83.00	256.39	341.98	465.72	180.02	339.66	
	Section3	98.74	268.99	301.19	482.01	162.02	292.31	
r2 (μ m)	Section1	37.91	162.56	64.74	178.73	58.44	159.70	0.00506 **
	Section2	43.20	146.49	72.24	144.85	60.62	163.56	
	Section3	35.57	169.43	66.36	129.95	51.15	155.89	
Expert 2								
d1 (μ m)	Section1	461.63	368.90	600.44	357.35	578.65	436.46	0.00475 **
	Section2	411.37	356.28	510.31	350.69	592.05	391.90	
	Section3	408.59	429.95	583.41	339.36	552.68	423.07	
d2 (μ m)	Section1	487.84	380.99	664.64	334.8	612.24	532.67	0.33588
	Section2	468.05	403.48	582.39	405.96	562.76	556.23	
	Section3	363.75	682.42	567.68	455.13	537.00	463.04	
r1 (μ m)	Section1	56.76	276.06	347.75	462.42	150.19	331.35	0.00544 **
	Section2	40.03	284.21	345.64	478.24	162.18	326.84	
	Section3	35.75	273.09	307.92	478.54	162.02	314.14	
r2 (μ m)	Section1	48.48	199.18	67.27	213.48	80.75	185.69	0.00504 **
	Section2	26.87	215.29	83.85	179.20	91.68	213.69	
	Section3	22.87	189.90	83.85	190.30	83.82	203.44	

Table S5. Results of social dominance tube test of PAS1^{w/m} vs. PAS1^{w/w} mice.

Cage number ^a	No. of PAS1 ^{w/m} vs. No. of PAS1 ^{w/w}	Winning rate of PAS1 ^{w/m}	Winning rate of PAS1 ^{w/w}	Age at group-housing (weeks)	Weight at group-housing (g)	Housed before tube test (weeks) ^b	Age at tube test (weeks)	Weight at tube test (g)
Cage 1	2:2	100%	0%	7.7	19.5-21.7	5.0	12.7	22.8-24.0
Cage 2	2:2	100%	0%	7.4	19.8-22.3	5.0	12.4	24.0-25.6
Cage 3	2:2	50%	50%	7.4-7.7	22.1-23.8	5.0	12.4-12.7	26.3-29.3
Cage 4	2:2	50%	50%	7.4-7.7	21.0-22.5	5.0	12.4-12.7	24.4-27.8
Cage 5	2:2	100%	0%	10.4	22.6-24.2	2.7	13.1	23.8-28.2
Cage 6	2:2	100%	0%	10.4	24.2-26.7	2.7	13.1	24.5-27.3
Cage 7	2:2	100%	0%	7.7-8.4	19.5-23.4	3.1	10.9-11.6	22.2-26.8
Cage 8	3:3	67%	33%	8.9-9.7	23.0-26.4	2.1	11.0-11.9	24.7-27.9
Cage 9	4:4	69%	31%	12.7-13.0	24.0-27.8	3.6	16.3-16.6	27.2-30.6
Cage 10	4:4	69%	31%	14.7-15.0	25.0-30.3	3.6	18.3-18.6	27.0-30.1
Cage 11	4:4	81%	19%	9.7-10.4	21.3-24.3	4.1	13.9-14.6	22.5-28.7
Summary		75.6%	24.4%					

^aMale mice with the same genotype were not paired. There were no female mice in cages 1 to 4.

^bThe exact time to acquire a stable rank was not examined in this study, but it was known to be less than the duration of housing time before tube test.

Table S6. Results of social dominance tube test of PAS1^{c/m} vs. PAS1^{c/c} mice.

Cage number ^a	No. of PAS1 ^{c/m} vs. No. of PAS1 ^{c/c}	Winning rate of PAS1 ^{c/m}	Winning rate of PAS1 ^{c/c}	Age at group-housing (weeks)	Weight at group-housing (g)	Housed before tube test (weeks) ^b	Age at tube test (weeks)	Weight at tube test (g)
Cage 1	2:2	0%	100%	11.6-11.7	24.8-27.3	3.4	15.0-15.1	27.4-29.6
Cage 2	2:2	0%	100%	11.6-11.7	23.2-24.6	3.4	15.0-15.1	22.8-26.5
Cage 3	2:2	0%	100%	9.6-9.9	23.0-24.4	3.3	12.9-13.1	25.8-26.9
Cage 4	2:2	0%	100%	9.6-9.9	19.7-22.6	3.3	12.9-13.1	23.1-25.5
Cage 5	2:2	0%	100%	9.1-9.6	18.8-22.1	3.1	12.3-12.7	22.5-24.6
Cage 6	2:2	0%	100%	9.1	21.2-23.4	3.9	13.0	23.0-26.3
Cage 7	2:2	0%	100%	9.1	20.1-21.1	3.9	13.0	22.5-23.6
Summary		0.0%	100.0%					

^aMale mice with the same genotype were not paired.

^bThe exact time to acquire a stable rank was not examined in this study, but it was known to be less than the duration of housing time before tube test.

Table S7. Results of social dominance tube test of PAS1^{-m} vs. PAS1^{-/-} mice.

Cage number	No. of PAS1 ^{-m} vs. No. of PAS1 ^{-/-}	Winning rate of PAS1 ^{-m}	Winning rate of PAS1 ^{-/-}	Age at group-housing (weeks)	Weight at group-housing (g)	Housed before test (weeks)	Age at tube test (weeks)	Weight at tube test (g)	Time to achieve stable social hierarchy
Cage 1	2:2	73%	27%	9.4-11.1	23.8-25.4	4.3	13.7-15.4	27.1-29.7	Unstable during the examined period of time.
Cage 2	2:2	45%	55%	9.4-9.6	21.9-23.5	4.3	13.7-13.9	24.2-28.9	
Cage 3	2:2	58%	42%	9.4	22.8-24.5	2.7	12.1	24.5-26.1	
Cage 4	2:2	68%	32%	7.9-8.7	21.1-22.5	4.0	11.9-12.7	23.7-25.2	
Cage 5	2:2	38%	62%	7.9-8.1	22.6-24.7	4.0	11.9-12.1	25.7-28.8	
Cage 6	2:2	88%	12%	7.9-8.7	23.1-25.7	4.0	11.9-12.7	26.9-29.9	
Summary		58.8%	41.2%						

Male mice with the same genotype were not paired.
 Average winning rates of PAS1^{-m} and PAS1^{-/-} in 10 consecutive days are shown.

Table S8. Results of social dominance tube test of PAS1^{-/-} mice.

Cage number	No. of PAS1 ^{-/-}	Age at group-housing (weeks)	Weight at group-housing (g)	Housed before tube test (weeks)	Age at tube test (weeks)	Weight at tube test (g)	Time to achieve stable social hierarchy
Cage 1	4	9.3-9.9	22.4-24.1	3.7	13.0-13.6	25.9-28.1	Unstable during the examined period of time.
Cage 2	4	9.3-9.9	24.0-25.4	3.7	13.0-13.6	27.7-29.5	
Cage 3	4	9.3-9.9	25.5-26.0	3.7	13.0-13.6	27.7-28.7	

Table S9. List of primers.

Experiments	Primers	Note
Cell transfection	hPAS1_Fx:CCGctcgagCTGCCTAGGAAGAGGAAGGA hPAS1_Rx:CCGctcgagAACCTGCCTTTTGTGGGAGG	
	mPAS1_Fx:CCGctcgagCTGCCTAGGAAGAGGAAGGA mPAS1_Rx:CCGctcgagACCCTGTGTTTTGTGGAAGG	
	cowPAS1_Fx:CCGctcgagCTGCCTAGGAAAAGGAAAAGA cowPAS1_Rx:CCGctcgagAACCTGCCTTCTGTGGGAGG	XhoI site built in
	wPAS1_Fx:CCGctcgagTTGCCTATAAAAATGAAGGA wPAS1_Rx:CCGctcgagAACCTGTATTTTGTAGTAGG	
	cPAS1_Fx:CCGctcgagTTGCCTATAAAAAGAAGAA cPAS1_Rx:CCGctcgagAACCTGTATTTTGTATAGG	
	miniPro_F:agcttTAGAGGGTATATAATGGAAGCTCGACTTCCAGA miniPro_R:agcttCTGGAAGTCGAGCTTCCATTATATACCCTCTAA	HindIII site built in
	RVP3_F:CTAGCAAAATAGGCTGTCCC PGL411_R:CCATGGTGGCTTTACCAACA	For verification of uptake of the plasmid carrying the reporter gene
	hPAS1_Fs:ACGCgtcgacCTGCCTAGGAAGAGGAAGGA hPAS1_Rs:ACGCgtcgacAACCTGCCTTTTGTGGGAGG	
	cPAS1_Fs:ACGCgtcgacTTGCCTATAAAAAAGAAGAA cPAS1_Rs:ACGCgtcgacAACCTGTATTTTGTATAGG	Sall site built in
	CF:TGCGGGCCTCTTCGCTATTA CR:TGAGGAGCAGTCTTTGATT	For verification of uptake of the plasmid carrying the reporter gene
Genotyping of ES cell targeting mouse	KO_P1:CATACTCCAAGAGTAACATCCCTGC KO_P2:GAATCGCCAACTAATTGACGCTGCA KO_P3:AGAGAATAGGAACTTCGTACCC	For PAS1 ⁻ model
	KI_P1:TTGTTCTGAGTTAGTCACGGTGGCC KI_P2:GGGTACGAAGTTCCCTATTCTCT KI_P3:AAACGCAGCCTAGAGAAATGCA	For PAS1 ^w and PAS1 ^c models
	InternalControl_F:CAACCACTTACAAGAGACCCGTA InternalControl_R:GAGCCCTTAGAAATAACGTTCCACC	
	Lhx2_F:GCCGAGAAAGCGCAAGAGT Lhx2_R:TGTTCAGCATCGTTCTCGTTACA	
	Lhx2_203F: GCTGCCGAGGGCTCACGAAG Lhx2_203R: CTGCCAGCAGGTAGTAGCGG Gapdh_F:CGTGTTCTACCCCAATGT	
RT-qPCR		

Gapdh_R: TGTCATCATACTTGGCAGGTTTCT

Gm27197_F: AAGCGGGCGCCCAGATTCT

Gm27197_R: CGCAGAGCCCTCCAGGATG

Dennd1a_F: TTTGATGACCTCCAGAGCCT

Dennd1a_R: CATCACCTGTGGTTGTAGAG

Table S10. Key resources table

REAGENT or RESOURCE	SOURCE	IDENTIFIER
Antibodies		
Anti-LHX2 Antibody	Millipore	ABE1402 (RRID:AB_2722523)
ALEXA FLUOR 488 goat anti-rabbit IgG (H+L)	Thermo Scientific	A11034 (RRID:AB_2576217)
Chemicals		
N,N,N',N'-Tetrakis(2-Hydroxypropyl)ethylenediamine	ALDRICH	122262
Agarose	Biowest	111860
MEM, NEAA, powder	Gibco	41500034
Trypsin (0.25%), phenol red	Gibco	15050057
Opti-MEM® I Reduced Serum Medium	Gibco	51985042
PureLink® Quick Plasmid Miniprep Kit	Invitrogen	K210010
SlowFade® Diamond Antifade Mountant with DAPI	Molecular Probes	S36964
FuGENE® HD Transfection Reagent	Promega	E2311
Dual-Glo® Luciferase Assay System	Promega	E2920
Dual-Luciferase® Reporter Assay System	Promega	E1910
HiSpeed Plasmid Maxi Kit (25)	Qiagen	12663
QIAGEN Plasmid Mini Kit (25)	Qiagen	12123
Tissue-Tek® O.C.T. Compound	SAKURA	4583
Paraformaldehyde	Sangon	A500684
Fetal Bovine Serum	SIGMA	12007C
Fast Green FCF Dye	SIGMA	F7252
Triton™ X-100	SIGMA	T9284
4', 6-Diamidino-2-phenylindole dihydrochloride	SIGMA	D8417-1MG
Takara MiniBEST Agarose Gel DNA Extraction Kit	TaKaRa	9762
MiniBEST Universal RNA Extraction Kit	TaKaRa	9767
PrimeScript RT-PCR Kit	TaKaRa	RR014A
Takara Ex Taq® Hot Start Version	TaKaRa	RR006A
FastDigest® HindIII	Thermo Scientific	FD0504
FastDigest® XhoI	Thermo Scientific	FD0694
FastAP Thermosensitive Alkaline Phosphatase	Thermo Scientific	EF0654
GeneGreen Nucleic Acid Dye	TIANGEN	RT210
DNA Marker I	TIANGEN	MD101-02
T4 DNA Ligase	TIANGEN	RT406
DH5α	TIANGEN	CB101-01
TIANquick Midi Purification Kit	TIANGEN	DP204
RNAstore Reagent	TIANGEN	DP408-02
pGM-T Cloning Kit	TIANGEN	VT202-01
TransStart® FastPfu DNA Polymerase	TransGen	AP221

Trans1-T1 Phage Chemically Competent Cell	TransGen	CD501
TransScript® II All-in-One First-Strand cDNA Synthesis SuperMix for qPCR	TransGen	AH341-01
TransStart® Top Green qPCR SuperMix	TransGen	AQ131-02
Bovine Serum Albumin , Lyophilized Powde	VETEC	V900933
Sucrose	VETEC	V900116
Urea	VETEC	V900119
Triethanolamine	VETEC	V900257
Consumables		
Thermo Scientific™ Nunc™	Thermo Scientific	142475
Assay Plate, 96 Well, No Lid	COSTAR	3362
LightCycler® 480 Multiwell Plate 96, white	Roche	04729692001
4IN THINWALL GL 1.0 OD/.75 ID	WPI	TW100F-4
Microloader 20µl	Eppendorf	5242856.003
Equipments		
Microplate reader	Bio-Tek	Synergy H1
Inverted fluorescence Microscope	Zeiss	Axio observer Z1
Micropipette Puller	SUTTER INSTRUMENT	MODEL P-2000
Microinjection pump	HARVARD APPARATUS	Pump 11 Elite
Stereoscopic microscope	Zeiss	Stemi 2000-C
3mm-diameter L-shaped electrode	BEX	LF613P3
In vivo electroporator	BEX	CUY21EDIT II
Stereo fluorescence microscope	Zeiss	AXIO Zoom.V16
Real-time quantitative PCR instrument	Roche	LightCycler® 480
Light sheet fluorescence microscopy	Zeiss	Lightsheet Z.1
Rota-rod	Shanghai Mobile Datum Information Technology Co.,LTD / Ugo basile	RD1123RS-G / Code: 47650
Experimental Models: Organisms/Strains		
Mouse: FVB (transgenic mouse enhancer assays)	Cyagen	http://www.cyagen.com/us/en/
	Cyagen	http://www.cyagen.com/us/en/
Mouse: C57BL/6	Shanghai Model Organisms Center,Inc	http://www.shmo.com.cn/English/

Mouse: C57BL/6 PAS1 ^{-/-} (mouse PAS1 knock-out)	This project (donated)	NM-KO-190421
Mouse: C57BL/6 PAS1 ^{w/w} (wallaby PAS1 knock-in)		NM-KI-190001
Mouse: C57BL/6 PAS1 ^{c/c} (chicken PAS1 knock-in)		NM-KI-190002
Plasmids for cell and chicken embryos transfection		
pGL4.11 vector	Promega	E6661
pGL4.74 reporter vector	Promega	E6921
miniPro-pGL4.11 reporter vector (miniPro-luc2P)		
hPAS1-miniPro-pGL4.11 reporter vector		
mPAS1-minoPro-pGL4.11 reporter vector	This project	N/A
cowPAS1-miniPro-pGL4.11 reporter vector		
wPAS1-miniPro-pGL4.11 reporter vector		
cPAS1-miniPro-pGL4.11 reporter vector		
PUC19 reporter vector	TransGen	N/A
pCAG-mCherry reporter vector	Addgene	41583 (RRID:Addgene_41583)
pCAG-EGFP reporter vector	This project	N/A
TK-EGFP reporter vector	Provided by Dr. Naihe Jing	N/A
TK-mCherry reporter vector		
hPAS1-TK-EGFP reporter vector	This project	N/A
cPAS1-TK-mCherry reporter vector		
Oligonucleotides		
Primers for PAS1, see Table S9	This project	N/A
Primers for Genotyping of ES cell targeting mouse, see Table S9	This project	N/A
Primers for RT-qPCR, see Table S9	This project	N/A
Recombinant DNA		
Hsp68-LacZ vector		
hPAS1-Hsp68-LacZ reporter vector		
mPAS1-Hsp68-LacZ reporter vector		
wPAS1-Hsp68-LacZ reporter vector	This project	N/A
cPAS1-Hsp68-LacZ reporter vector		
ES cell targeting vector, mm9-KOS141218, PAS1 ⁻		
ES cell targeting vector, mm9-KIS141215, PAS1 ^w		
ES cell targeting vector, mm9-galGal3, PAS1 ^c		
Cell Lines		
Mouse: Neuro2a	Cell Bank of CAS	TMC29
Human: HEK-293	Cell Bank of CAS	GNHu43
Software		
KungFuPanda	This project	http://www.picb.ac.cn/evo

		igen/softwares/
eGPS ⁵		http://www.egps-software.net/
Vision4D 2.12.3	Arivis	http://www.arivis.com/
BLASTN ¹²		https://blast.ncbi.nlm.nih.gov/Blast.cgi
MULTIZ ¹³		http://www.bx.psu.edu/miller_lab
UCSC Kent utilities		http://hgdownload.cse.ucsc.edu/admin/jksrc.zip

References

- 1 Daily, J. L. *et al.* Adeno-associated virus-mediated rescue of the cognitive defects in a mouse model for Angelman syndrome. *PLoS one* **6**, e27221 (2011).
- 2 Ogawa, N., Hirose, Y., Ohara, S., Ono, T. & Watanabe, Y. A simple quantitative bradykinesia test in MPTP-treated mice. *Res Commun Chem Pathol Pharmacol* **50**, 435-441 (1985).
- 3 Li, W.-H., Ellsworth, D. L., Krushkal, J., Chang, B. H. & Hewett-Emmett, D. Rates of nucleotide substitution in primates and rodents and the generation-time effect hypothesis. *Mol Phylogenet Evol* **5**, 182-187 (1996).
- 4 Saitou, N. & Nei, M. The neighbor-joining method: a new method for reconstructing phylogenetic trees. *Mol Biol Evol* **4**, 406-425 (1987).
- 5 Yu, D. *et al.* eGPS 1.0: comprehensive software for multi-omic and evolutionary analyses. *Natl Sci Rev* **6**, 867-869 (2019).
- 6 Weinreb, C. & Raphael, B. J. Identification of hierarchical chromatin domains. *Bioinformatics* **32**, 1601-1609 (2016).
- 7 Rao, S. S. P. *et al.* A 3D map of the human genome at kilobase resolution reveals principles of chromatin looping. *Cell* **159**, 1665-1680 (2014).
- 8 Kerpedjiev, P. *et al.* HiGlass: web-based visual exploration and analysis of genome interaction maps. *Genome Biol* **19**, 125 (2018).
- 9 Hernandez-Miranda, L. R., Muller, T. & Birchmeier, C. The dorsal spinal cord and hindbrain: From developmental mechanisms to functional circuits. *Dev Biol* **432**, 34-42 (2017).
- 10 Creyghton, M. P. *et al.* Histone H3K27ac separates active from poised enhancers and predicts developmental state. *Proc Natl Acad Sci USA* **107**, 21931-21936 (2010).
- 11 Mele, M. *et al.* The human transcriptome across tissues and individuals. *Science* **348**, 660-665 (2015).
- 12 Altschul, S. F. *et al.* Gapped BLAST and PSI-BLAST: a new generation of protein database search programs. *Nucleic Acids Res* **25**, 3389-3402 (1997).
- 13 Blanchette, M. *et al.* Aligning multiple genomic sequences with the threaded blockset aligner. *Genome Res* **14**, 708-715 (2004).